

## Semiannual NO<sub>2</sub> plumes during the monsoon transition periods over the central Indian Ocean

T. Kunhikrishnan, Mark G. Lawrence, and Rolf von Kuhlmann

Department of Atmospheric Chemistry, Max Planck Institute for Chemistry, Mainz, Germany

Andreas Richter, Annette Ladstätter-Weißmayer, and John P. Burrows

Institute of Environmental Physics and Remote Sensing, University of Bremen, Bremen, Germany

Received 12 December 2003; revised 19 February 2004; accepted 23 March 2004; published 30 April 2004.

[1] In this study we identify recurring plumes of tropospheric NO<sub>2</sub> originating from Africa and Indonesia during the monsoon transition periods over the central Indian Ocean (CIO, 5°N–30°S, 55°E–95°E), based on GOME satellite observations and global model (MATCH-MPIC) simulations. Despite the relatively short lifetime of NO<sub>x</sub>, these strong plumes can develop due to the pronounced anti-cyclonic circulation over the CIO, and the weak maritime convection, which limits vertical mixing. Model results indicate that the plumes are mainly transported in the middle troposphere (MT). Thus, the CIO in the Southern Hemisphere (SH) is not always as pristine as found in INDOEX during the winter monsoon. **INDEX TERMS:** 0300 Atmospheric Composition and Structure; 0368 Atmospheric Composition and Structure: Troposphere—constituent transport and chemistry; 0933 Exploration Geophysics: Remote sensing; 1620 Global Change: Climate dynamics (3309); 1610 Global Change: Atmosphere (0315, 0325). **Citation:** Kunhikrishnan, T., M. G. Lawrence, R. von Kuhlmann, A. Richter, A. Ladstätter-Weißmayer, and J. P. Burrows (2004), Semiannual NO<sub>2</sub> plumes during the monsoon transition periods over the central Indian Ocean, *Geophys. Res. Lett.*, 31, L08110, doi:10.1029/2003GL019269.

### 1. Introduction

[2] Current knowledge of atmospheric chemistry over the Indian Ocean is limited due to the scarcity of long-term observations. The region is dynamically and chemically active because of differential heating between the continents and the ocean, high humidity and the large and increasing tropical anthropogenic emissions. The Indian Ocean is characterized by a monsoon circulation, i.e., the seasonal reversal of winds, associated with north-south oscillations of the Intertropical Convergence Zone (ITCZ). During the monsoon periods, the winds are mainly meridional and the zonal winds are weaker over equatorial Indian Ocean. Much of our present understanding of the regional chemistry relies on the results of the Indian Ocean Experiment (INDOEX) during the winter monsoon periods of 1995–1999, which contrasted the relatively polluted northern hemisphere (NH) with the more pristine SH air [Lelieveld *et al.*, 2001]. Less is known about the chemistry during the intermonsoon periods, when zonal winds dominate the circulation.

[3] An important component of tropospheric chemistry is NO<sub>x</sub> (NO + NO<sub>2</sub>), which catalyzes O<sub>3</sub> production and

influences OH and the tropospheric oxidization efficiency. The main maritime NO<sub>x</sub> sources are long-range transport of continental emissions, lightning and ships. Recent studies have used satellite instruments such as GOME (Global Ozone Monitoring Experiment) to examine isolated NO<sub>2</sub> plume episodes over marine regions [Ladstätter-Weißmayer *et al.*, 2003; Stohl *et al.*, 2003; Wenig *et al.*, 2003]. In this study, we use GOME data from 1996–2000 and output from the Model of Atmospheric Transport and Chemistry-Max Planck Institute for Chemistry version (MATCH-MPIC) to document the presence of semiannual tropospheric NO<sub>2</sub> plumes over the central Indian Ocean (CIO) and to investigate their interannual and intraseasonal variability.

### 2. Descriptions of GOME and MATCH-MPIC

#### 2.1. GOME

[4] GOME is on the ESA ERS II satellite, launched in April 1995. It provides global monitoring of NO<sub>2</sub> through nadir observations of solar backscatter at 0.31 nm spectral resolution between 423–451 nm, where NO<sub>2</sub> has strong absorption features. Global coverage is achieved every 3 days after 43 orbits with a spatial resolution of 40 × 320 km<sup>2</sup>. The NO<sub>2</sub> retrieval assumes clear sky conditions (considers pixels with cloud cover <0.1), a maritime aerosol, a surface albedo of 0.05 and a constant mixing ratio of NO<sub>2</sub> below 1.5 km; details are given by Burrows *et al.* [1999] and Richter and Burrows [2002]. The tropospheric NO<sub>2</sub> column is obtained by subtracting the NO<sub>2</sub> column over the Pacific Oceanic reference sector (170°W–180°W) at the same latitude from the total NO<sub>2</sub> column at the longitude being retrieved. This, together with the uncertainty in the NO<sub>2</sub> fit (<5% [Richter and Burrows, 2002]), determines the detection limit of ~5 × 10<sup>14</sup> molec/cm<sup>2</sup>. The accuracy is additionally limited by uncertainties due to the presence of clouds, and the error in the air mass factor. As a standard air mass factor has been used in this study, NO<sub>2</sub> columns over water may be overestimated, in particular in the presence of low clouds, which may contribute to differences between the model results and measurement; note, however, that this can only enhance or degrade a signal, but will not create a plume where no enhancement is present in the raw data.

#### 2.2. MATCH-MPIC

[5] MATCH-MPIC is a global 3D chemistry-transport model. The present study uses version 3.1, employed by Lawrence *et al.* [2003], at a horizontal resolution of T21 (64 × 32 grid cells) with 28 vertical levels up to ~2.7 hPa.

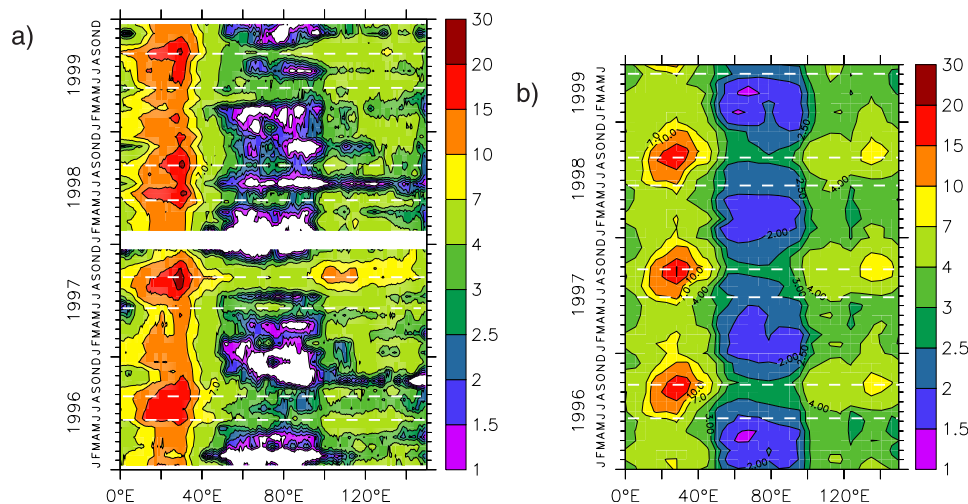


**Figure 1.** Tropospheric NO<sub>2</sub> column (in  $10^{14}$  molecules/cm<sup>2</sup>) averaged for 5°N–30°S from (a) GOME (b) MATCH; only the overlapping period (1996–1999) is plotted; results are similar for the full data sets of each; see Figure 2 for a map of the region.

The meteorology component is driven by NCEP/NCAR reanalysis data and simulates transport by advection, convection and dry turbulent mixing. The photochemistry component represents the sources and sinks of O<sub>3</sub> and 55 related gases. Details are given by *Rasch et al.* [1997], *Lawrence et al.* [1999], and *von Kuhlmann et al.* [2003]. We examined the model output at 10:30 local time, corresponding to the GOME overpasses, for January 1993 through July 1999. The tropospheric NO<sub>2</sub> column from the model used here is computed as the integrated value from the surface to 100 hPa.

### 3. GOME Satellite Observations and Model Simulation of NO<sub>2</sub> Plumes Over the CIO

[6] The observed tropospheric NO<sub>2</sub> column over the CIO (averaged over 5°N–30°S) from GOME (Figure 1a) shows a semi-regular plume of enhanced NO<sub>2</sub> levels stretching across the entire CIO (marked with dashed white lines), generally strongest during the monsoon transition periods (MTP) of April–May (onset-MTP) and September–October (withdrawal-MTP). There is a strong interannual variability. The most intense plumes are during the withdrawal-MTP, corresponding to the most intense biomass burning periods over the source regions of Africa and Indonesia. These regular plumes are one of the rare instances where monthly-mean GOME NO<sub>2</sub> observations above the detection limit can be repeatedly found over large remote ocean regions (see the blue and green contours in Figure 2).

[7] MATCH-MPIC is able to reproduce these plumes well during the withdrawal-MTP (Figure 1b), with the exception that the simulation shows relatively little interannual variability, due to the use of climatological monthly biomass burning emissions. MATCH-MPIC also produces the plumes during the onset-MTP, but these are generally strongly underestimated, extending only to ~60°E on the west side and ~80°E on the east side. In the model, weaker NO<sub>2</sub> plumes mainly start to be visible from April–May, and

continue during the monsoon months and become strongest in September–October (see auxiliary material<sup>1</sup>: material-1). The weakness of the plumes during the onset-MTP and their continuation during the summer monsoon likely results from errors in the modeled meteorology over the oceanic region, which in turn results from the scarcity of maritime observations, a general problem with many of the reanalysis products for the Indian Ocean [*Schott and McCreary*, 2001]. Furthermore, based on the comparison, the emissions over Africa are apparently low in MATCH. The decay of the NO<sub>2</sub> plume on the African side is too slow in MATCH, while on the Indonesian side it is generally faster than observed by GOME. This is likely to be due to errors in OH or in the outflow rates, which cannot be determined without further in situ observations. Despite the difficulties with the onset-MTP plumes, the monthly mean NO<sub>2</sub> columns averaged over four sub domains (5°N–30°S latitude; 20°E–40°E, 100°E–120°E, 60°E–80°E and 80°E–100°E longitude) are relatively well correlated between MATCH-MPIC and GOME ( $r = 0.56$ – $0.71$ ). In addition, both MATCH-MPIC and GOME CIO NO<sub>2</sub> columns have a coefficient of variation of 70–80%, which indicates the strong seasonal variability in NO<sub>2</sub>, mainly because of the occurrence of the plumes. Thus, we will make use of MATCH-MPIC to give a first impression of the detailed nature of the plumes, focusing particularly on the withdrawal-MTP. In the model analysis, we focus on NO<sub>x</sub> instead of NO<sub>2</sub> because the family NO<sub>x</sub> is being transported over larger distances in the atmosphere, since the equilibrium processes determining NO–NO<sub>2</sub> partitioning are much faster than the processes which affect the total NO<sub>x</sub> concentration.

[8] In the rest of this study we examine two questions with respect to the plumes: (i) What is the horizontal, vertical and temporal structure of the plumes, (ii) How are these plumes related to the regional meteorology and atmospheric chemistry?

### 4. Plume Structure

[9] The mean horizontal structure of the NO<sub>2</sub> plume from GOME during September 1997 is depicted in Figure 2. The

<sup>1</sup>Auxiliary material is available at <ftp://ftp.agu.org/apend/gl/2003GL019269>.

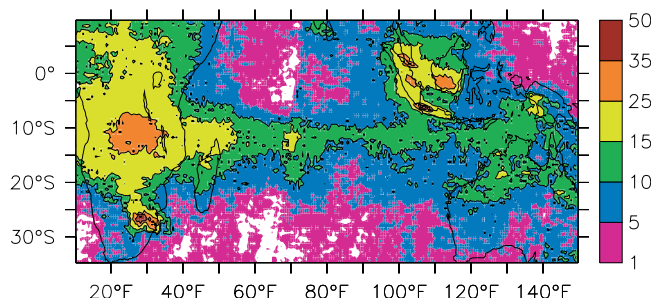


**Figure 2.** Horizontal structure of the NO<sub>2</sub> plume (in 10<sup>14</sup> molecules/cm<sup>2</sup>) from GOME for September 1997.

plumes extend across the CIO from Africa and Madagascar and converge with the outflow from the Indonesian region at 70°E–80°E and move further southeast towards Australia. An example of the typical instantaneous vertical structure of the plume computed by MATCH-MPIC (Figure 3) shows that the transport of enhanced NO<sub>x</sub> air masses across the southern CIO (10°S–30°S) is mainly in the MT with a notable enhancement in the upper troposphere (UT), which is partly from the stratosphere, and partly from convective outflow (these cannot be separated in our current model simulations). We have confirmed that the NO<sub>2</sub> column enhancement is also dominantly coming from the MT: for the CIO in September 1997, the contributions from the boundary layer and UT are relatively small (<1 × 10<sup>14</sup> molecules/cm<sup>2</sup>), while the main contributions come from the layers 850–700 hPa, 700–500 hPa, and 500–300 hPa (1.5–2, 2–3, and 1 × 10<sup>14</sup> molecules/cm<sup>2</sup>, respectively). On some occasions, the NO<sub>x</sub> plumes extend much deeper, from ~700 hPa up to as high as 250 hPa. To allow a better visualization of the structure and temporal evolution of the plumes we provide animations of NO<sub>x</sub> as well as NO<sub>2</sub> at different isobaric levels for September 1997 in the auxiliary material<sup>1</sup> (material-2 and material-3).

## 5. Chemical and Meteorological Conditions During the Intermonsoon Periods

[10] The interannual and intraseasonal variability of NO<sub>x</sub> is determined by the variability in three main factors; source strength, photochemical production and loss, and the transport patterns. The major NO<sub>x</sub> sources for the African plume during September and May consist of biomass burning, industry and lightning over southeast and central Africa [Fishman *et al.*, 1991; Thompson *et al.*, 2001; Wenig *et al.*,

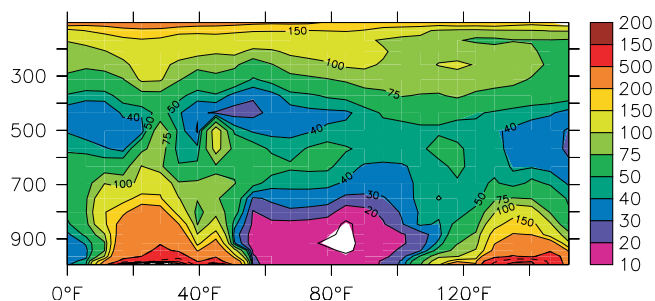


**Figure 3.** Vertical profile of NO<sub>x</sub> (in pptv) over the southern CIO from MATCH for 18 September 1997.

2003]; in September, biomass-burning emissions from Africa are expected to be more significant than lightning and industrial emissions and less significant during May. Over Indonesia, convection and lightning are very active during the transition periods, especially during September [Kita *et al.*, 2003], although there is a large interannual variability, especially enhanced biomass burning during dry El-Niño periods (e.g., September–October 1997).

[11] The degree of dispersion of NO<sub>2</sub> is determined by the wind speed and by the lifetime of NO<sub>x</sub> ( $\tau(\text{NO}_x)$ ), both of which vary with respect to space and time [Kunhikrishnan *et al.*, 2004]. Nevertheless, a rough estimate can be made of the expected extent of the plume. In the lower troposphere (LT),  $\tau(\text{NO}_x)$  can vary from several hours to at most a couple of days, while in the UT,  $\tau(\text{NO}_x) \approx 2\text{--}10$  days. Given the typical wind speed of  $\geq 10$  m/s in the MT (see below) the plume is expected to be prominent for about 2000–10,000 km ( $\sim 20^\circ\text{--}100^\circ$  longitude) in the MT across the CIO, while in the LT with wind speeds  $\leq 10$  m/s the expected extent will be less than 1000 km.

[12] Examples of the streamlines and zonal wind speeds for MT (0.501  $\sigma$ ) and UT (0.312  $\sigma$ ) circulations for September 1997 are given in Figure 4, showing a strong anticyclonic circulation over the CIO during September. In general, during September and May, in the LT (below 700 hPa), the winds are dominated by easterlies (with a wind speed of  $\sim 5$  m/s) from the equator to 20°S and weak westerly winds from 25°S to 30°S. Above 500 hPa, generally the winds are easterlies ( $\sim 10$  m/s) in the northern part of the CIO (10°S to 5°N) and the southern part of the CIO (10°S–30°S) above 700 hPa is occupied by strong westerly winds with speed of 10–30 m/s, increasing with altitude.

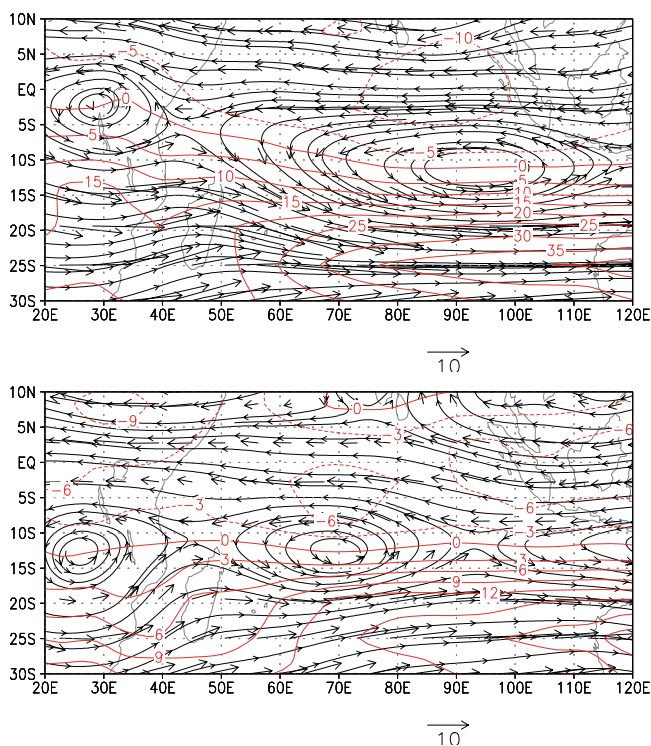


**Figure 4.** Zonal winds (red solid lines for westerly, dotted for easterly) and streamlines (in black) for 0.312  $\sigma$  (top) and 0.501  $\sigma$  (bottom) levels.

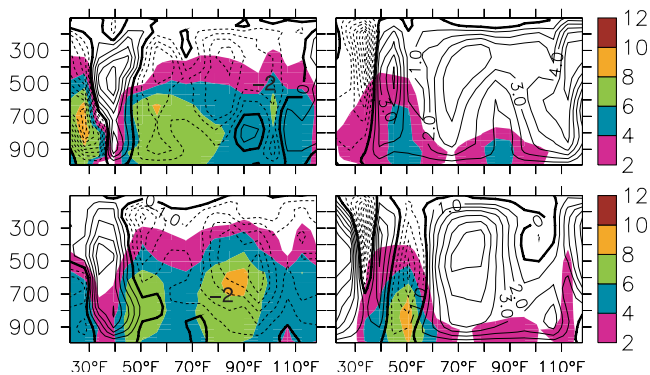


**Figure 5.** Vertical profile of convective mass flux (shaded in  $\text{g/m}^2/\text{s}$ ) and vertical velocity ( $d\eta/dt$ , in  $10^{-17}/\text{s}$ , solid contour lines represent subsidence and dotted lines upwelling) from MATCH at  $5^\circ\text{S}$  (left), and  $25^\circ\text{S}$  (right) for September 1997 (top) and May 1998 (bottom).

From 3-hourly model output for September 1997, we found that the zonal winds, especially westerlies, are dominant during the days in which enhanced plumes are present. The ridge of the anti-cyclone shifts gradually from being weakly present at  $25^\circ\text{S}$  in the LT at 800 hPa to being strong above 600 hPa, continuing to shift north to the equator at 200 hPa, so that the westerly wind zone broadens with altitude. Simultaneously, the easterlies from Indonesia to the north of the anti-cyclone are active, depending on the position of the ridge, which determines their extent over the CIO. This results in an effective plume transport in the MT across the CIO. During May, the divergent circulations are generally weaker and the ridge is centered from  $15^\circ\text{S}$ – $25^\circ\text{S}$  in the MT and becomes more intense above 400 hPa, where the ridge shifts northwards from  $15^\circ\text{S}$  to the equator (not shown). At the same time dominant cyclonic circulation can also be seen over the northeast CIO during this month. In general the oscillations and northeastward slope of the ridge with height in the latitudinal domain determine the strength and extent of zonal winds and their day-to-day variability on either side, which in turn determines the plume transport by westerly and easterly winds.

[13] Transport of continental surface sources to the MT and UT takes place by deep convection as well as by turbulent mixing and large-scale upwelling. Examples of the vertical transport components over the CIO based on the convective mass fluxes and vertical velocity ( $d\eta/dt$  in hybrid coordinates, representing large scale upward motion) computed with MATCH-MPIC are shown in Figure 5. Deep convection is mainly dominant over the continental source regions over Africa and Indonesia at  $5^\circ\text{S}$ – $5^\circ\text{N}$ , as well as around  $25^\circ\text{S}$  close to Africa and Madagascar, which enables the vertical uplifting of emissions from the LT at the continental source region to the MT and UT and transport across the CIO. The intensification of the plumes close to Madagascar (Figures 1 and 2) is due to the uplifting of additional emissions (especially from lightning) from this area. The convection is shallow over the CIO (especially during September 1997), which limits the dilution of air in the plumes with NO<sub>x</sub>-poor MBL air. During September, the subsidence induced by the divergent circulation covers a broad region from  $10^\circ\text{S}$  to  $25^\circ\text{S}$  (Figure 5) but is only over a

limited area during May close to  $25^\circ\text{S}$ . Most of the northern CIO ( $5^\circ\text{N}$ – $15^\circ\text{S}$ ) during May is influenced by moderate convection up to 400 hPa, which dilutes the NO<sub>x</sub> within the MT of the CIO with NO<sub>x</sub>-poor MBL air, thus reducing its average lifetime [Lawrence *et al.*, 2003]. Thus, even though the dispersion by westerly winds is strong during May, this dilution hinders accumulation of NO<sub>x</sub> and an effective transport over the CIO, resulting in weaker plumes during May.

## 6. Conclusions

[14] In this study we have used GOME satellite observations of the tropospheric NO<sub>2</sub> column together with output from the 3D chemistry-transport model MATCH-MPIC to demonstrate the existence of and examine the characteristics of semiannual plumes of enhanced NO<sub>2</sub> that stretch across the CIO during the monsoon transition periods. The circulation features and the regional chemistry are favorable for effective plume transport and accumulation of polluted air masses over the CIO. The plume is generally strongest during the withdrawal-MTP because of the enhancement of NO<sub>x</sub> emissions from biomass burning and stronger anti-cyclonic circulation, which strengthens the outflow and extent of zonal winds. It is also present during the onset-MTP, though less pronounced, mainly due to weaker emissions along with the cyclonic circulation in the northeastern CIO and active shallow maritime convection. Our findings of recurring plumes during the MTPs, as observed from space and simulated by the model, suggest that the CIO is not always as pristine as found during INDOEX and is polluted, especially in the MT, by emissions from continental regions of the SH. It is recommended that further field studies, especially during the transition periods, be carried out to explore the extent of this pollution and the air quality of this region.

[15] **Acknowledgments.** We acknowledge support for MATCH from Phil Rasch, NCAR, Boulder, USA and funding for the work at the MPI from BMBF, Germany, project 07-ATC-02. The first author is grateful to India Meteorological Department for granting leave for his study at MPIC, Mainz.

## References

- Burrows, J. P., et al. (1999), The Global Ozone Monitoring Experiment (GOME): Mission concept and first scientific results, *J. Atmos. Sci.*, *56*, 151–175.
- Fishman, J., K. Fakhruzzaman, B. Cros, and D. Naganga (1991), Identification of widespread pollution in the Southern Hemisphere deduced from satellite analyses, *Science*, *252*, 1693–1696.
- Kita, K., et al. (2003), Photochemical production of ozone in the upper troposphere in association with cumulus convection over Indonesia, *J. Geophys. Res.*, *108*(D3), 8400, doi:10.1029/2001JD000844.
- Kunhikrishnan, T., M. G. Lawrence, R. von Kuhlmann, A. Richter, A. Ladstätter-Weissenmayer, and J. P. Burrows (2004), Analysis of tropospheric NO<sub>x</sub> over Asia using the Model of Atmospheric Transport and Chemistry (MATCH-MPIC) and GOME-satellite observations, *Atmos. Environ.*, *38*, 581–596.
- Ladstätter-Weissenmayer, A., et al. (2003), Transport and build-up of tropospheric trace gases during the MINOS campaign: Comparisons of GOME, in situ air craft measurements and MATCH-MPIC-data, *Atmos. Chem. Phys.*, *3*, 1887–1902.
- Lawrence, M. G., P. J. Crutzen, P. J. Rasch, B. E. Eaton, and N. M. Mahowald (1999), A model for studies of tropospheric photochemistry: Description, global distributions and evaluation, *J. Geophys. Res.*, *104*, 26,245–26,277.
- Lawrence, M. G., R. von Kuhlmann, M. Salzmänn, and P. J. Rasch (2003), The balance of effects of deep convective mixing on tropospheric ozone, *Geophys. Res. Lett.*, *30*(18), 1940, doi:10.1029/2003GL017644.

- Lelieveld, J., et al. (2001), The Indian Ocean Experiment: Widespread air pollution from south and southeast Asia, *Science*, 291, 1031–1036.
- Rasch, P. J., N. M. Mahowald, and B. E. Eaton (1997), Representations of transport, convection and the hydrologic cycle in chemical transport models: Implications for the modeling of short lived and soluble species, *J. Geophys. Res.*, 102, 28,127–28,138.
- Richter, A., and J. P. Burrows (2002), Retrieval of tropospheric NO<sub>2</sub> from GOME measurements, *Adv. Space Res.*, 29, 1673–1683.
- Schott, F., and J. P. McCreary Jr. (2001), The monsoon circulation of the Indian Ocean, *Prog. Oceanogr.*, 51, 1–123.
- Stohl, A., et al. (2003), Rapid intercontinental air pollution transport associated with a meteorological bomb, *Atmos. Chem. Phys.*, 3, 969–985.
- Thompson, A. M., J. C. Witte, R. D. Hudson, H. Guo, J. R. Herman, and M. Fujiwara (2001), Tropical tropospheric ozone and biomass burning, *Science*, 291, 2128–2132.
- von Kuhlmann, R., M. G. Lawrence, P. J. Crutzen, and P. J. Rasch (2003), A model for studies of tropospheric ozone and nonmethane hydrocarbons: Model description and ozone results, *J. Geophys. Res.*, 108(D9), 4294, doi:10.1029/2002JD002893.
- Wenig, M., N. Spichtinger, A. Stohl, G. Held, S. Beirle, T. Wagner, B. Jähne, and U. Platt (2003), Intercontinental transport of nitrogen oxide pollution plumes, *Atmos. Chem. Phys.*, 3, 387–393.

---

J. P. Burrows, A. Ladstätter-Weißmayer, and A. Richter, Institute of Environmental Physics and Remote Sensing, University of Bremen, Postfach 330440, D-28344 Bremen, Germany.

T. Kunhikrishnan, M. G. Lawrence, and R. von Kuhlmann, Department of Atmospheric Chemistry, Max Planck Institute for Chemistry, D-55128 Mainz, Germany. (kunhi@mpch-mainz.mpg.de)